

# Single Molecule Fluorescence Analysis of Branch Migration of Holliday Junctions: Effect of DNA Sequence

Mikhail A. Karymov,\* Alexey Bogdanov,\*<sup>†</sup> and Yuri L. Lyubchenko\*

\*Department of Pharmaceutical Sciences, University of Nebraska Medical Center, Nebraska Medical Center, Omaha, Nebraska 68198-6025; and <sup>†</sup>Department of Molecular Biophysics, Research Institute of Physics, St. Petersburg State University, Petrodvorets, St. Petersburg, Russia

**ABSTRACT** The Holliday junction is a central intermediate in various genetic processes including homologous, site-specific recombination and DNA replication. Recent single molecule FRET experiments led to the model for branch migration as a stepwise stochastic process in which the branch migration hop is terminated by the folding of the junction. In this article, we studied the effect of the sequence on Holliday junction dynamics and branch migration process. We show that a GC pair placed at the border of the homologous region almost prevents the migration into this position. At the same time, insertion of a GC pair into the middle of the AT tract does not show this effect, however when the junction folds at this position, it resides at this position much longer time in comparison to the folding at AT pairs. Two contiguous GC pairs do not block migration as well and generally manifest the same effect as one GC pair—the junction when it folds resides at these positions for a relatively long time. The same elevated residence time was obtained for the design with the homology region that consists of only GC pairs. These data suggest a model for branch migration in which the sequence modulates the overall stochastic process of the junction dynamics and branch migration by the variability of the time that the junction dwells before making a migration hop.

## INTRODUCTION

Branch migration of the Holliday junction (HJ) is a key process in homologous and site-specific genetic recombination (1,2). However, our knowledge about this process is very limited, due primarily to the lack of appropriate methods. The kinetics of spontaneous branch migration was studied in the early works of Panyutin et al. (3) and Panyutin and Hsieh (4,5) in which the rate of branch migration was obtained. These studies proposed the model for branch migration, suggesting that unfolding of the Holliday junction is needed for branch migration. These studies also showed the effect of  $Mg^{2+}$  cations that decrease the rate of branch migration. The model and effect of  $Mg^{2+}$  cations are supported by our recent single molecule AFM experiments in which unfolding of the junction was imaged directly by the time lapse AFM imaging in aqueous solutions. The junction unfolding model was in line with our recent single molecule fluorescence study in which branch migration was observed in real-time at the single molecule level (6). According to these data the junction flips between folded and unfolded conformations. Branch migration occurs when the junction unfolds, and this process stalls when the junction folds. Divalent cations stabilize folded conformations increasing dramatically the folded conformation residence time. Regardless of this recent progress, many questions related to the detailed mechanism of branch migration still remain unanswered. One of these

questions is the role of the sequence. The early kinetics data (4,5,7) were analyzed in the framework of one-dimensional Brownian model with no effect of the sequence. A more rigorous analysis was carried out in a recent theoretical article by Bruist and Myers (8) where the importance of the sequence heterogeneity was emphasized, but this effect was not included in the model because of the lack of appropriate data. The effect of the sequence on the thermodynamics of the HJ folding was analyzed by Zhang et al. (9), Fu and Seeman (10), and Sun et al. (11). This group developed and used symmetric immobile double crossover designs to evaluate the effect of the bases adjacent to the junction on the efficiency of the migration step. These studies showed a significant effect of flanking sequences on the junction stability, suggesting that the sequence had to be taken into account in modeling of the kinetics of branch migration.

Our previous sp-FRET experiments were carried out with a sequence containing alternating AT pairs. To evaluate the role of the sequence heterogeneity, specifically the role of GC pairs imbedded into AT type sequence, we designed a set of mobile HJ constructs by placing GC pairs at different locations within the alternating AT sequence. The data show a strong effect of the sequence on the branch migration pattern, but in a rather unexpected way. A single GC pair at the border of the homologous ATAT sequence practically blocks the migration to this position. However, an internal GC pairs allow for migration, but the junction folds and dwells at GC pairs a longer time compared to the residence times at AT pairs. The application of the results obtained to the mechanisms of HJ branch migration is discussed.

*Submitted December 13, 2007, and accepted for publication March 25, 2008.*

Address reprint requests to Yuri L. Lyubchenko, Dept. of Pharmaceutical Sciences, University of Nebraska Medical Center, 986025 Nebraska Medical Center, Omaha, NE 68198-6025. Tel.: 402-559-5320; Fax: 402-559-9543; E-mail: [ylyubchenko@unmc.edu](mailto:ylyubchenko@unmc.edu).

Editor: David P. Millar.

© 2008 by the Biophysical Society  
0006-3495/08/08/1239/09 \$2.00

doi: 10.1529/biophysj.107.127522

## MATERIALS AND METHODS

### Holliday junction design

Several sets of four oligonucleotides for assembly of mobile (m) and immobile (i) versions of HJ were synthesized (IDT, Coralville, IA). The oligonucleotides were internally amino-labeled for attachment of dyes. The sequences for oligonucleotides 1–4 are as follows:

#### ATATA

1. biotin-5'-TCTTTTGATAAGCTTGCAAGCATA TATAT CTCGTAA-TTTCGGTTAGGT.
2. 5'-ACCTAACCGGAAATTACGAG ATATA GATGCATGCAAGC-TTCACA.
3. 5'-TGTGAAGCTTGCA/iAmMC6T/GCATC TATAT AATACGT-GAGGCTAGGATC.
4. 5'-GATCCTAGGCCTCACGTATT ATATA TATGC/iAmMC6T/TGCAAGCTTATCA.

#### CTATA

1. biotin-5'-TCTTTTGATAAGCTTGCAAGCATA GATAT CTCGTA-ATTTCCGGTTAGGT.
2. 5'-ACCTAACCGGAAATTACGAG ATATC GATGCATGCAAGC-TTCACA.
3. 5'-TGTGAAGCTTGCA/iAmMC6T/GCATC GATAT AATACGTG-AGGCCTAGGATC.
4. 5'-GATCCTAGGCCTCACGTATT ATATC TATGC/iAmMC6T/TGCAAGCTTATCA.

#### ATGTA

1. biotin-5'-TCTTTTGATAAGCTTGCAAGCATA TACAT CTCGTA-ATTTCCGGTTAGGT.
2. 5'-ACCTAACCGGAAATTACGAG ATGTA GATGCATGCAAGC-TTCACA.
3. 5'-TGTGAAGCTTGCA/iAmMC6T/GCATC TACAT AATACGTG-AGGCCTAGGATC.
4. 5'-GATCCTAGGCCTCACGTATT ATGTA TATGC/iAmMC6T/TGCAAGCTTATCA.

#### ACGTA

1. biotin-5'-TCTTTTGATAAGCTTGCAAGCATA TGCAT CTCGTA-ATTTCCGGTTAGGT.
2. 5'-ACCTAACCGGAAATTACGAG ATGCA GATGCATGCAAGC-TTCACA.
3. 5'-TGTGAAGCTTGCA/iAmMC6T/GCATC TGCAT AATACGTG-AGGCCTAGGATC.
4. 5'-GATCCTAGGCCTCACGTATT ATGCA TATGC/iAmMC6T/TGCAAGCTTATCA.

#### GCGCG

1. biotin-5'-TCTTTTGATAAGCTTGCAAGCATA GCGCG CTCGTA-ATTTCCGGTTAGGT.
2. 5'-ACCTAACCGGAAATTACGAG GCGCG GATGCATGCAAGC-TTCACA.
3. 5'-TGTGAAGCTTGCA/iAmMC6T/GCATC GCGCG AATACGTG-AGGCCTAGGATC.
4. 5'-GATCCTAGGCCTCACGTATT GCGCG TATGC/iAmMC6T/TGCAAGCTTATCA.

All sequences are named by the exchanging sequence of oligonucleotide 2 in the direction from 5' to 3' end.

Immobile junctions were designed in such a way that the donor–acceptor distances in entire set covered the range of branch migration of mobile HJ. The sequences to ensemble set of six immobile HJs to build calibration curve

allowed to make the junctions with 10, 12, 14, 16, 18, and 20 basepair (bp) separations between the dyes and the designs were named by this number. To eliminate potential effect of the sequence on the optical properties of the dyes via the dye–bases interaction, the sequences around the donor and acceptor dyes in all designed remained identical.

#### 10 bp

1. biotin-5'-TCTTTTGATAAGCTTGCAAGCATA ATATA CTCGTA-ATTTCCGGTTAGGT.
2. 5'-ACCTAACCGGAAATTACGAG TATAT GATGCATGCAAGC-TTCACA.
3. 5'-TGTGAAGCTTGCA/iAmMC6T/GCATC TATAT AATACGTG-AGGCCTAGGATC.
4. 5'-GATCCTAGGCCTCACGTATT ATATA TATGC/iAmMC6T/TGCAAGCTTATCA.

#### 12 bp

1. biotin-5'-TCTTTTGATAAGCTTGCAAGCATA CTATA CTCGTA-ATTTCCGGTTAGGT.
2. 5'-ACCTAACCGGAAATTACGAG TATAC GATGCATGCAAGC-TTCACA.
3. 5'-TGTGAAGCTTGCA/iAmMC6T/GCATC GATAT AATACGTG-AGGCCTAGGATC.
4. 5'-GATCCTAGGCCTCACGTATT ATATG TATGC/iAmMC6T/TGCAAGCTTATCA.

#### 14 bp

1. biotin-5'-TCTTTTGATAAGCTTGCAAGCATA CATAT CTCGTA-ATTTCCGGTTAGGT.
2. 5'-ACCTAACCGGAAATTACGAG ATAAC GATGCATGCAAGC-TTCACA.
3. 5'-TGTGAAGCTTGCA/iAmMC6T/GCATC GTAAT AATACGTG-AGGCCTAGGATC.
4. 5'-GATCCTAGGCCTCACGTATT ATTTG TATGC/iAmMC6T/TGCAAGCTTATCA.

#### 16 bp

1. biotin-5'-TCTTTTGATAAGCTTGCAAGCATA GCTAT CTCGTA-ATTTCCGGTTAGGT.
2. 5'-ACCTAACCGGAAATTACGAG ATTCC GATGCATGCAAGC-TTCACA.
3. 5'-TGTGAAGCTTGCA/iAmMC6T/GCATC GGATT AATACGTG-AGGCCTAGGATC.
4. 5'-GATCCTAGGCCTCACGTATT AAAGC TATGC/iAmMC6T/TGCAAGCTTATCA.

#### 18 bp

1. biotin-5'-TCTTTTGATAAGCTTGCAAGCATA GCTAT CTCGTA-ATTTCCGGTTAGGT.
2. 5'-ACCTAACCGGAAATTACGAG AACTC GATGCATGCAAGC-TTCACA.
3. 5'-TGTGAAGCTTGCA/iAmMC6T/GCATC GAGTA AATACGTG-AGGCCTAGGATC.
4. 5'-GATCCTAGGCCTCACGTATT TTAGC TATGC/iAmMC6T/TGCAAGCTTATCA.

#### 20 bp

1. biotin-5'-TCTTTTGATAAGCTTGCAAGCATA GAGAT CTCGT-AATTTCCGGTTAGGT.
2. 5'-ACCTAACCGGAAATTACGAG TCAAC GATGCATGCAAGC-TTCACA.
3. 5'-TGTGAAGCTTGCA/iAmMC6T/GCATC GTTGA AATACGTG-AGGCCTAGGATC.

#### 4. 5'-GATCCTAGGCCTCACGTATT ATCTC TATGC/iAmMC6T/TGCAAGCTTATCA.

Oligonucleotides 3 and 4 in all designs were labeled with succinimide esters of Cy3 or Cy5 dyes (GE Healthcare, Chalfont St. Giles, UK) according to the protocol provided by the company. Labeled oligonucleotides were purified by reverse-phase high-performance liquid chromatography and four-way junctions (Fig. 1 *b*) were prepared by the annealing protocol described elsewhere (6). The yield of the annealing reaction determined by gel electrophoresis was ~80–90%.

### Experimental setup and FRET efficiency estimation

The original time trajectories of the fluorescence intensity were acquired as described previously using the same confocal type instrument (6,12).

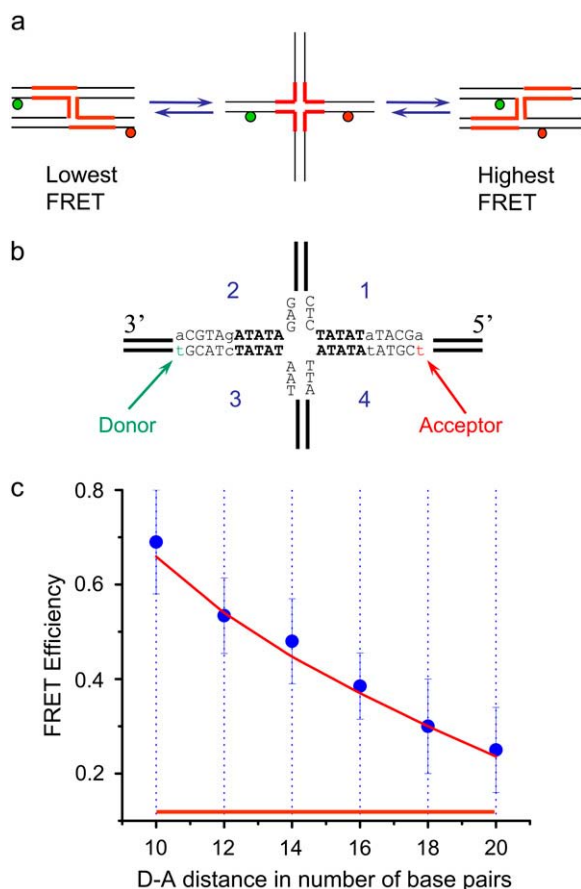


FIGURE 1 (a) Diagram explaining principle of branch migration and folding for mobile HJ design used in single-pair FRET studies. Homologous exchanging regions are indicated with thick red lines. (b) Schematic of central regions of HJ including donor and acceptor dyes attached. The design with ATATA exchanging sequence (**boldface**) and the longest D–A distance is shown on a figure. All sequences are called by the exchanging sequence of oligo2 in the direction from 3' to 5' end. Corresponding sequences are designated in the Materials and Methods section. The single nonhomologous basepairs of interest are designated with the small letters. (c) The dependence of FRET values of immobile HJ junctions on the donor–acceptor distances in basepairs. Error bars show the SD calculated from the multiple measurements. The red line is a best smooth fit to the measured points. The region of HJ mobility covering all six possible folded positions is shown as a red horizontal bar.

Cleaned glass coverslips were treated sequentially with 1 mg/ml biotinylated BSA (Sigma, St. Louis, MO) in pH 7.5 TES buffer (10 mM Tris-HCl, 150 mM NaCl, 1 mM EDTA) for 10 min, rinsed with TES buffer, 0.5  $\mu$ M solution of streptavidin in the same buffer for 10 min, and rinsed with TES buffer. A 50 pM solution of biotinylated HJ in TES buffer was added and incubated for ~10 min. Measurements were carried out in TNM buffer (10 mM Tris-HCl, 100 mM NaCl, 10 mM MgCl<sub>2</sub>) containing oxygen-scavenging system based on glucose oxidase and catalase (13). Experiments were carried out in two independent series of measurements. The first series of measurements was done with using 1%  $\beta$ -mercaptoethanol as a free-radicals quencher, the second set of the data was obtained with the use of 1.5 mM Trolox (Sigma-Aldrich, USA) in imaging buffer described in Rasnick et al. (14). Lifetime of the single molecules before photobleaching increased substantially in the last series of measurements producing time trajectories as long as 40 s. Both series of measurements gave very similar patterns and lifetimes at each migration step.

Apparent FRET efficiencies were calculated according to formula  $E = I_A / (I_D + I_A)$ . Fluorescence intensities of donor ( $I_D$ ) and acceptor ( $I_A$ ) were obtained by subtracting background counts from the raw intensities and correcting for crosstalk between the two detection channels according to Ha (15).

### Plateau search and assignment algorithm

Only single-molecule time trajectories of fluorescence changes above the threshold intensity level were analyzed. The threshold value was determined based on the noise level estimated from the standard deviation (SD) of the fluorescence intensity fluctuation for long plateaus for mobile and immobile four-way junctions. This value did not exceed ~0.06 at 6 ms time interval binning. A value of 0.12 (two SD values for the noise level) was chosen as a minimal discernible step size. Averaged data were obtained using the following algorithm. The Holliday junction is considered to remain at the same migration step in adjacent time bins 1 and 2 if the FRET-efficiency difference  $|E_1 - E_2| < 0.12$ . The mean-plateau efficiency is calculated as  $\bar{E} = (E_1 + E_2) / 2$ . The plateau continues to the third time bin if  $|E_3 - \bar{E}| < 0.12$ . This procedure repeats for subsequent bins and the new mean efficiency  $\bar{E}$  is determined according to the general formula for the mean. If the FRET efficiency at the later time in two consequential bins differs by  $>0.12$  from the mean efficiency of the plateau ( $|E_{i+1} - \bar{E}| > 0.12$  and  $|E_{i+2} - \bar{E}| > 0.12$ ), the algorithm stops the plateau search routine, calculates the mean efficiency for the plateau value and duration, and then starts over the search of a new plateau. Single data points with an efficiency difference exceeding 0.12 are replaced with the previous mean plateau value.

The assignment of the plateau positions to a number of basepairs between the dyes was carried out with the use of the calibration curve shown on Fig. 1 *c* (a red line obtained as a best fit to the measured points). Positions of the plateaus in a number of basepairs were calculated based on proximity of their FRET efficiency values to the FRET values of the nearest intersect of the vertical dashed blue line with the smooth fit.

## RESULTS AND DISCUSSION

### Holliday junction design

Similar to our previous study (6), the designs for this project were made in such a way that the homologous sequence was located in the central part of the constructs. The branch migration region of the mobile HJ is limited to the two 5-bp homologous sequences on both sides of the junction indicated with the thick red lines in Fig. 1 *a*. A schematic for the design is shown in Fig. 1 *b* where the variable part of the junction is designated in boldface font. The homologous sequences were made by inserting of GC pairs into alternating

ATATA stretches. One design is a GCGCG repeat. The homology between the arms of the junction is interrupted by incorporation of nonhomologous basepairs. The lengths of nonhomology regions on labeled arms were 1 bp and 5 bp, as even one nonhomologous basepair is able to block spontaneous branch migration (16). The other two HJ arms were completely nonhomologous beyond the exchanging regions. Donor (Cy5) and acceptor (Cy3) dyes were placed on the opposite junction arms, allowing us to monitor branch migration via measurements of FRET. We have shown that this method of labeling is not compromised by the global conformation changes such as junction folding (6) enabling us to follow branch migration primarily.

### Stepwise branch migration process

During a one-basepair migration step, the distance between the donor and acceptor changes by two basepairs. We had assumed earlier that this change in the distance can be detected by FRET using the setup described above (6). To prove it directly, and correlate the change of FRET efficiency with the dye-to-dye distance, a set of immobile HJs with the dyes attached at the positions corresponding in Fig. 1 *a* to distances 10, 12, 14, 16, 18, and 20 bp were constructed. Note that this set of HJs covers the entire range of branch migration of mobile HJs. The junctions were end-anchored to the glass surface via biotin-streptavidin links. All measurements were carried out in TNM buffer containing 10 mM of  $Mg^{2+}$  cations.

The FRET values for all these designs were measured and the data averaged over dozens of single molecule traces are plotted in Fig. 1 *c*. The highest value of the FRET efficiency corresponds to the smallest D–A distance (Fig. 1 *a*, *right scheme*) and the efficiency drops monotonously on increasing the donor-acceptor distance. Note that the D–A separation is indicated in basepairs corresponding to the sequence of the junction rather than the geometric distance between the dyes. The latter requires the knowledge of the exact junction geometry in both folded and unfolded states. Thus, these data directly support our earlier assumption that FRET values can be measured over the entire homology range of the mobile HJ designs with one basepair distance increment.

### Sequence dependent migration and folding of the Holliday junctions

Fig. 2 *a* shows the time trace for the design consisting of homologous ATATA sequences. The blue line in the figure shows the raw data for FRET efficiency binned over 6 ms time intervals. This time trajectory has a stepwise pattern that is seen clearly in the red line that was obtained by averaging the original data and implying the plateau searching algorithm described previously (6). The FRET time trajectories have a clear-cut stepwise pattern; this pattern is similar to one observed in our previous work (6). We interpreted the pla-

teaus as the residing of the HJ in folded states whereas each vertical line was assigned to the migration hop or the branch migration step, which is the transition of the junction from one folded state to another. Availability of the calibration curve (Fig. 1 *c*) allows us to test this interpretation. Horizontal green dotted lines on Fig. 2 *a* correspond to FRET values for each basepair within the homology region. These values were obtained from the calibration curve in Fig. 1 *c*. It is seen clearly that the positions of plateaus on the time trace practically coincide with the positions of corresponding dotted lines allowing us to assign the FRET value for the plateau to the appropriate position of the branch within the homology region. Using the calibration curve, we modified the time trajectory in such a way that the FRET values were replaced with the donor–acceptor distances measured in number of basepairs. In this procedure, the plateau FRET value was replaced by the closest green dotted line (see Materials and Methods for specifics). For example, plateau with FRET efficiency of 0.439 shown at the beginning of time trajectory on Fig. 2 *a* was replaced with the green dotted line at 0.45 efficiency, which corresponds to 14 bp distance; the next plateau with 0.303 efficiency was replaced with the dotted line at 0.30 efficiency corresponding to 18 bp distance; short plateau with 0.451 efficiency was substituted with the green dotted line at 0.45, which also matching to 14 bp distance between donor and acceptor and so on. As a result, the time trajectory in Fig. 2 *a* is transformed into the stepwise time trajectory shown in Fig. 2 *b*.

The graph in Fig. 2 *b* illustrates clearly the basepairwise migration of the junction from the longest distance (20 bp) the shortest one (10 bp). The dinucleotide sequence corresponding to the one-basepair branch migration step is indicated to the right of the time trace. This time graph shows clearly the variability of the step size. The hop varies from 1 bp (e.g., a hop at  $\sim 2.2$  s) to 5 bp ( $\sim 2.4$  s); the latter value corresponds to the entire length of the homology region. The lengths of plateaus (the residence times) vary between 10–100 ms that correspond very well to the values obtained in the study by Karymov et al. (6). The data for the residence times averaged over a series of independent experiments is shown in Fig. 2 *c*. On this graph, the mean residence time values for each position of the junction within the homologous region are shown. These data show that the mean residence time values are  $\sim 50$  ms, although there is some decrease of the residence time for the positions of the junction branch close to the ends of the homology regions; so the largest residence times correspond to the positions of the junction in the middle of the sequence.

Fig. 3 *a* shows the time trace for another design in which a GC pair was placed at end of the homology region closest to the donor. Similar to the previous graph, the blue line corresponds to the binned raw data, averaged data are shown with a red line, and dotted green lines show the FRET values for each basepair within the homologous region obtained from the calibration curve (Fig. 1 *c*). Similar to Fig. 2 *b*, Fig.

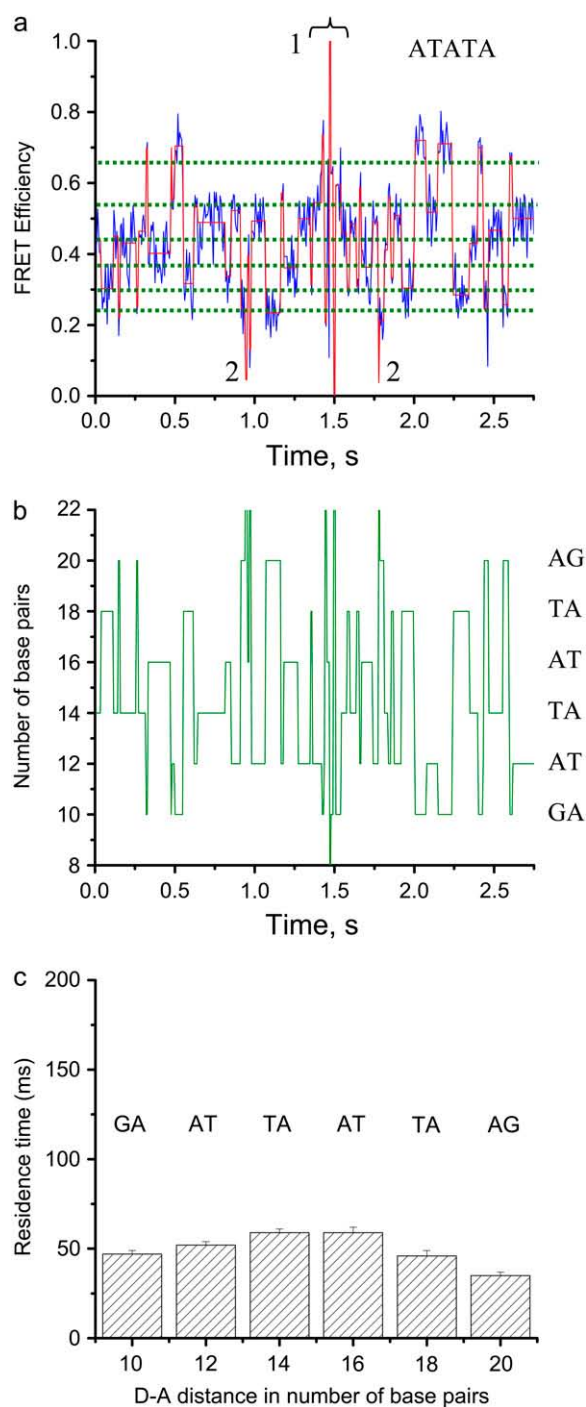


FIGURE 2 Single pair FRET (sp FRET) data for mobile Holliday junctions with ATATA exchanging sequence. (a) Time dependence of spFRET efficiency (blue line). Original intensity data were binned with 6 ms binning interval. The red line is produced by averaging of the blue line data using the algorithm described in Materials and Methods section. This procedure allows revealing and visualizing of the plateaus on the time trajectories. The green horizontal dotted lines are the FRET efficiency values obtained from the calibration plot corresponding to each possible folded position of the junction. The dark states on these trajectories for donor and acceptor indicated with (1) and (2) respectively were not included into the analysis. (b) Time trajectory of the donor-acceptor distances in number of basepairs. The oligo2 dinucleotide sequences in the direction of 3' → 5' flanking the

3 b shows the time trace replotted against the donor-acceptor distance in number of basepairs. Again, plateau assignments were done based on a best fit to the calibration curve values. For example, the plateau at 1.3 s (Fig. 3 a) is slightly closer by its mean FRET value to the green dashed line corresponding to 12 bp distance (CT dinucleotide in Fig. 3 b) and is assigned by the program to this position. At the same time, the next plateau (~1.4 s) is closer to the 14 bp line (TA dinucleotide in Fig. 3 b). The stepwise pattern is very similar to the previous sequence shown on Fig. 2 b, but the highest FRET value (*top dotted line*) corresponding to the smallest D-A distance do not appear on this time trajectory. Other experiments were consistent with this finding and they show that folding of the junction at the shortest donor-acceptor distance are relatively rare events. This position corresponds to the position of the junction at the inserted GC pairs. The dependence of the residence time values averaged over a series of time traces are shown in Fig. 3 c. There is some variability in the residence times for different positions of the junction within the homology region with values slightly higher than for the previous design. The sequences above the histogram indicate the dinucleotide of the folded state. Note a small residence time for the junction folded at the GC pair (10 bp for the donor-acceptor distance).

The time trace in Fig. 4 a corresponds to the branch migration experiment for the junction with the sequence in which one GC pair was placed within the AT-stretch. The replotted time trace (Fig. 4 b) shows that the junction resides much longer at the GC pair positions (indicated with arrows) in comparison to all other positions of the branch. This effect is clearly seen in Fig. 4 c, where the averaged data on the residence times are summarized. The mean value for the residence time for branch folded at the GC-pair position is three times higher compared to the branch position at AT pairs.

Fig. 5 a summarizes results of the experiments carried out with the design containing two adjacent GC pairs within the AT stretch (see Fig. S1 in Supplementary Material, [Data S1](#) for time traces data). This graph shows that folding of the junction at GC pairs increases the residence times, but the effect extends to adjacent AT basepairs as well. For example, the residence time of the AT pair located to the left of CG pair is twice of the value obtained for the previous design (Fig. 4 c). The same effect is observed for the AT pair located to the right of the CG pair.

It is instructive to compare these results with the design consisting of GC pairs only. Such a design was made, with the FRET data analyzed and the results of the experiments are summarized in Fig. 5 b (see Fig. S2 in [Data S1](#) for time

junction point at each migration step are indicated at corresponding steps positions. (c) The distribution of the mean residence time values for each branch position for each folded state. Averaged data for 18 molecules with ~4000 folded states total are shown. The error bars show SE.



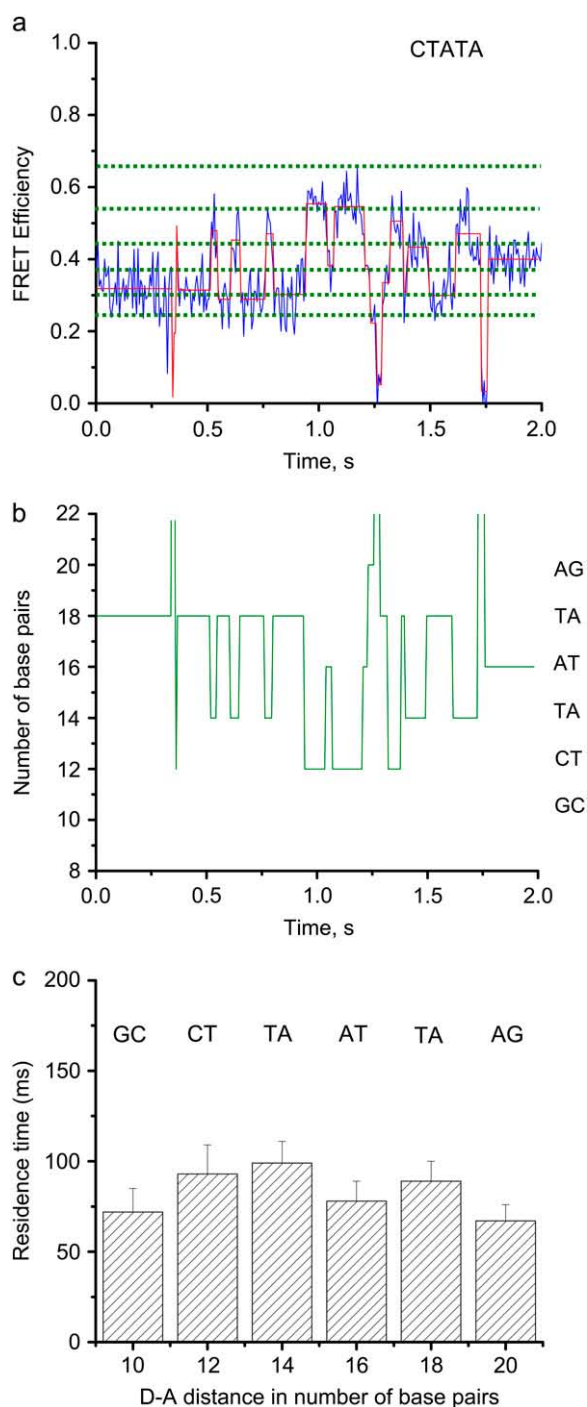


FIGURE 3 The FRET efficiencies and plateau positions time trajectories for mobile Holliday junctions with CTATA exchanging sequence. (a) Time dependence of spFRET efficiency (blue line). The red line and green dotted lines have the same meaning as in Fig. 2. (b) Time trajectory of the donor-acceptor distances in number of basepairs (steps are designated as explained in the legend of Fig. 2). (c) Distribution of the mean residence time versus migration step. Averaged data for 14 molecules with  $\sim 350$  folded states total are shown. The error bars show SE.

traces). This histogram shows that the residence times for the junction folded at locations proximate to the left of end of the sequence (positions 10–16) are high and the values ( $\sim 150$  ms) are almost the same as observed for previous designs when folding occurs at GC pairs (Figs. 4 c and 5 a). The drop of the residence time values for distantly located folded state positions of the junction was unexpected. The designs used in these experiments have different sequences at the borders of the homologous sequence. Indeed, the 10-bp homology region was separated from adjacent homologous region by a nonhomologous basepair. The other side of the 10-bp homologous region consisted of a long stretch of a nonhomologous sequence. Therefore, we hypothesized that the asymmetry in the histogram can be due to the asymmetry of the HJ designs that gives some preference to one end of the junction compared to the other one. According to the data of Panyutin and Hsieh (4) and Biswas et al. (16), even 1 bp heterology should be sufficient to terminate branch migration. However, our data indicate that this may not be the case suggesting that a single nonhomologous basepair can allow migration at some extent. The rationale for such a hypothesis stems from the chemical modification data that show that the nucleotides at the branch of the four-way junction have elevated accessibility to chemical and enzymatic probes (3,17,18). In addition, computer modeling of HJs shows that the basepairing of the nucleotides located at the junction are not perfectly paired (19,20).

To test this hypothesis, we designed a junction in which the same homologous 10-bp region is flanked by nonhomologous regions consisting of at least five basepairs (see Fig. S3 in Data S1 for schematics). The results of multiple experiments are summarized in Fig. 5 c. The residence time for the basepair at the proximate border of the homologous region drops dramatically. Importantly, the residence time for this very first GC pair indicated by an arrow is  $\sim 70$  ms that is almost three times smaller than the value obtained for the previous design with one nonhomologous basepair at the border (Fig. 5 b). The distribution of the residence times has a clear-cut maximum corresponding to the junction folded in the middle. The highest residence time value corresponds to the position of the second GC pair of the homologous insert. The residence times for the GC pairs away from the plot maximum have low values (50–80 ms). Interestingly, these values are very close to ones obtained for the design containing AT pairs only (Fig. 2).

These findings suggest that two factors, GC content and the location of the junction relative to the homology range, contribute to the dynamics and branch migration of the junction. The insertion of GC pairs increases the lifetime of folded states, but only if they are at least one basepair away from the homology border. The proximity of the homology border decreases the residence time of the folded state for GC pairs approaching them to the values for AT pairs.

The real-time single molecule observations showed an interesting effect of the DNA sequence on the branch migration

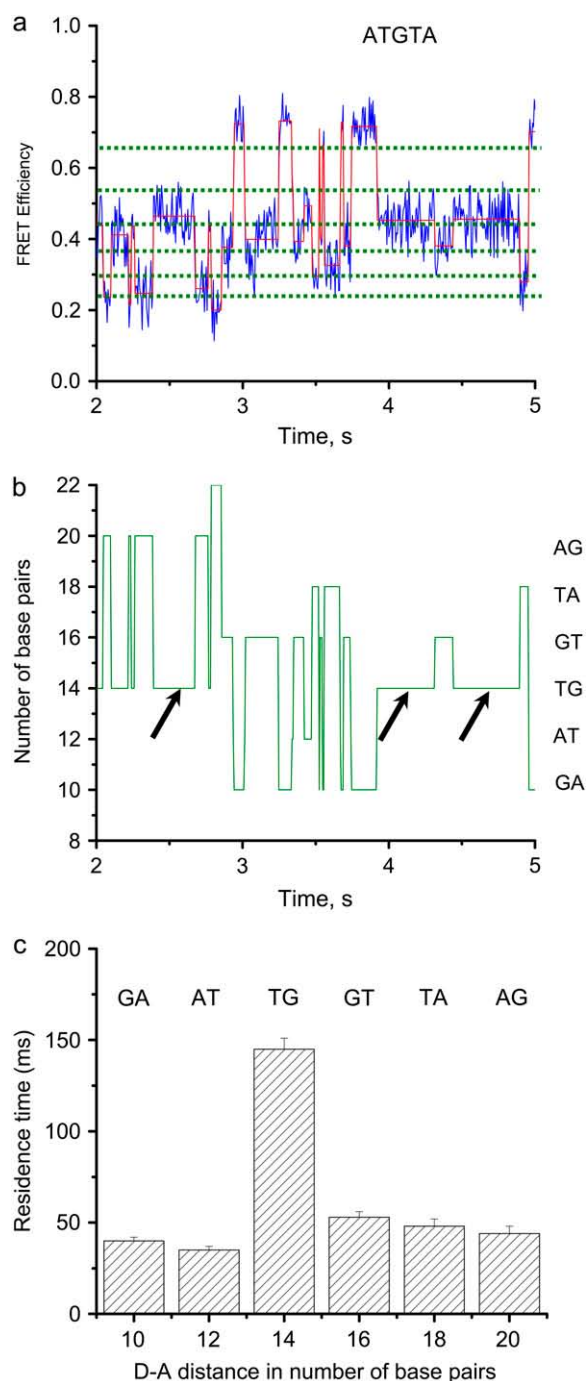


**FIGURE 4** The FRET efficiencies and plateau positions time trajectories for mobile Holliday junctions with ATGTA exchanging sequence. (a) Time dependence of spFRET efficiency (blue line) of mobile Holliday junction. The red line and green dotted lines have the same meaning as in the previous figures. (b) Time trajectory of the donor-acceptor distances in number of basepairs. Black arrows pointed to time trajectory section corresponding to the folding at the GC pair. (c) Distribution of the mean residence time versus migration step. Averaged data for 14 molecules with ~2300 folded states total have been analyzed. The error bars show SE.

pattern. One can anticipate that thermodynamically more stable GC pairs compared to the less stable AT pairs may impede branch migration due to the lower probability for opening of the basepairs required for the junction migration. Indeed, we observed that the branch rarely migrates to a GC pair, but only in the case when it is located at the end of the homology region. However, no such blockage was observed if GC pairs are located in the middle of the homology region. Instead, we observed a different effect of the sequence. The junction folds and resides considerably longer at GC pairs in comparison to AT basepairs. Similar long residence times are observed for the sequence containing GC pairs only. Moreover, the residence time values practically coincide for a singlet GC pair and GC dinucleotide. The residence times for terminal positions of the homologous regions are lower than for the folding of the junction within the region, and the effect is very pronounced for GC pairs compare to AT pairs. These observations suggest that the bases within the branch of the junction are structured in such a way that homologous and nonhomologous basepairs are accommodated differently into the branch.

Altogether, the data paint the following picture for spontaneous branch migration of the Holliday junction: the junction undergoes branch migration when it unfolds, and in this state, it can make a hop that is not necessarily one basepair, so the hop as large as several basepairs can be made. The migration hop is terminated by folding of the junction. There might be a conformational transition of the junction (folding) without a migration of the branch, although our hypothesis is that each unfolding event is accompanied by migration step. This model can be tested using more sophisticated three-color FRET experiments in which a third label is placed on one of the vertical arms. These experiments are currently in progress.

The data obtained show that migration stochastic process is modulated by the sequences that influence the time the junction resides in the folded state. The residence time is larger for GC pairs in comparison to AT pairs. Thus, the higher the GC content of the homologous region, the longer the time required for spontaneous junction migration over the entire region. Therefore, thermostable GC pairs decrease the overall migration rate, but not due to their lower basepair opening probability. Rather, the transition of the junction between the folded and unfolded conformations is the mechanism thereby the sequence modulates the branch migration process. The nonhomologous bases terminate branch migration, so the junction folds at the borders, but the residence time for these folded states is relatively short. Thus, the ends of the homology region play a role of the reflective borders. A single nonhomology basepair indeed terminates the migration process, although it permits the approaching of the branch to the very end of the homology region. Long nonhomology regions are needed to make a hard stop, even decreasing the probability of incorporation of terminal homologous basepairs into the branch. These data suggest that the sequence homology play as an important role in the

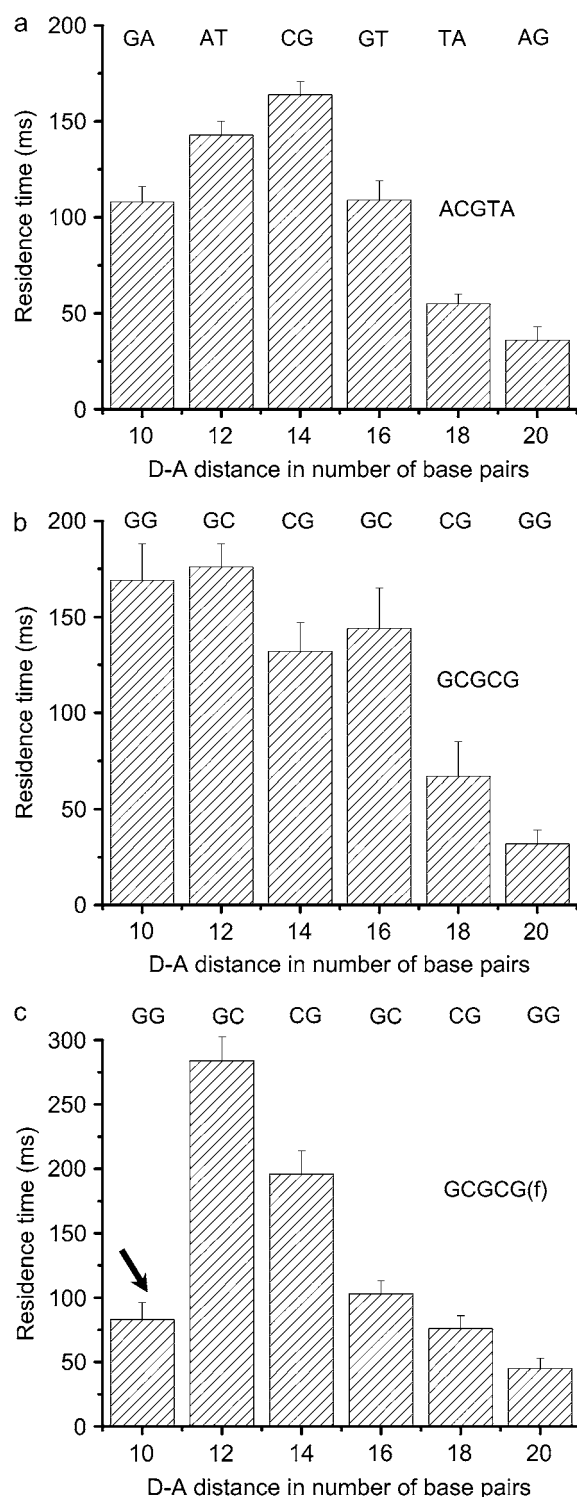


FIGURE 5 The distribution of the residence time values for the folded states for each position of the junction for different homologous sequences. (a) ACGTA (23 molecules, ~2600 plateaus), (b) GCGCG (13 molecules, ~500 plateaus), (c) GCGCG (34 molecules, ~1450 plateaus) indicate the homologous sequences for one DNA strand. Lower case f in (c) indicates elongated non-homologous flanks surrounding exchanging sequence, a whole HJ design with such flanks shown in Fig. S3 in Data S1. The arrow in histogram (c) points to the bar the height of which changed the most substantially on changing the sequences flanking the homologous region. The error bars show SE.

structure and dynamics of HJs. This finding is line with our early AFM imaging data of mobile HJ and cruciforms (21–25) and altogether they provide additional evidence to the difference in the structure and dynamics of immobile and mobile Holliday junctions. Further experiments and computer modeling are needed to elucidate this difference.

## SUPPLEMENTARY MATERIAL

To view all of the supplemental files associated with this article, visit [www.biophysj.org](http://www.biophysj.org).

We thank A. Krasnolobovtsev and L. Shlyakhtenko for valuable comments and fruitful discussions.

This work was supported by the National Institutes of Health grant GM0062235 and the National Science Foundation grant PHY-0615590, both to Y.L.L.

## REFERENCES

- Holliday, R. 1964. A mechanism for gene conversion in fungi. *Genet. Res.* 5:282–304.
- Leach, D. R. F. 1996. Genetic recombination. Oxford [England]; Cambridge, Mass., USA: Blackwell Science.
- Panyutin, I. G., I. Biswas, and P. Hsieh. 1995. A pivotal role for the structure of the Holliday junction in DNA branch migration. *EMBO J.* 14:1819–1826.
- Panyutin, I. G., and P. Hsieh. 1993. Formation of a single base mismatch impedes spontaneous DNA branch migration. *J. Mol. Biol.* 230:413–424.
- Panyutin, I. G., and P. Hsieh. 1994. The kinetics of spontaneous DNA branch migration. *Proc. Natl. Acad. Sci. USA.* 91:2021–2025.
- Karymov, M., D. Daniel, O. F. Sankey, and Y. L. Lyubchenko. 2005. Holliday junction dynamics and branch migration: single-molecule analysis. *Proc. Natl. Acad. Sci. USA.* 102:8186–8191.
- Robinson, B. H., and N. C. Seeman. 1987. Simulation of double-stranded branch point migration. *Biophys. J.* 51:611–626.
- Bruist, M. F., and E. Myers. 2003. Discrete and continuous mathematical models of DNA branch migration. *J. Theor. Biol.* 220:139–156.
- Zhang, S., T. J. Fu, and N. C. Seeman. 1993. Symmetric immobile DNA branched junctions. *Biochemistry.* 32:8062–8067.
- Fu, T. J., and N. C. Seeman. 1993. DNA double-crossover molecules. *Biochemistry.* 32:3211–3220.
- Sun, W., C. Mao, F. Liu, and N. C. Seeman. 1998. Sequence dependence of branch migratory minima. *J. Mol. Biol.* 282:59–70.
- Karymov, M. A., A. V. Krasnoslobodtsev, and Y. L. Lyubchenko. 2007. Dynamics of synaptic SfiI-DNA complex: single-molecule fluorescence analysis. *Biophys. J.* 92:3241–3250.
- Harada, Y., K. Sakurada, T. Aoki, D. D. Thomas, and T. Yanagida. 1990. Mechanochemical coupling in actomyosin energy transduction studied by in vitro movement assay. *J. Mol. Biol.* 216:49–68.
- Rasnik, L., S. A. McKinney, and T. Ha. 2006. Nonblinking and long-lasting single-molecule fluorescence imaging. *Nat. Methods.* 3:891–893.
- Ha, T. 2001. Single-molecule fluorescence resonance energy transfer. *Methods.* 25:78–86.
- Biswas, I., A. Yamamoto, and P. Hsieh. 1998. Branch migration through DNA sequence heterology. *J. Mol. Biol.* 279:795–806.
- Churchill, M. E., T. D. Tullius, N. R. Kallenbach, and N. C. Seeman. 1988. A Holliday recombination intermediate is twofold symmetric. *Proc. Natl. Acad. Sci. USA.* 85:4653–4656.



18. Sha, R., H. Iwasaki, F. Liu, H. Shinagawa, and N. C. Seeman. 2000. Cleavage of symmetric immobile DNA junctions by *Escherichia coli* RuvC. *Biochemistry*. 39:11982–11988.
19. von Kitzing, E., D. M. Lilley, and S. Diekmann. 1990. The stereochemistry of a four-way DNA junction: a theoretical study. *Nucleic Acids Res.* 18:2671–2683.
20. Srinivasan, A. R., and W. K. Olson. 1994. Computer models of DNA four-way junctions. *Biochemistry*. 33:9389–9404.
21. Shlyakhtenko, L. S., V. N. Potaman, R. R. Sinden, and Y. L. Lyubchenko. 1998. Structure and dynamics of supercoil-stabilized DNA cruciforms. *J. Mol. Biol.* 280:61–72.
22. Shlyakhtenko, L. S., P. Hsieh, M. Grigoriev, V. N. Potaman, R. R. Sinden, and Y. L. Lyubchenko. 2000. A cruciform structural transition provides a molecular switch for chromosome structure and dynamics. *J. Mol. Biol.* 296:1169–1173.
23. Lyubchenko, Y. L., L. S. Shlyakhtenko, V. N. Potaman, and R. R. Sinden. 2002. Global and local DNA structure and dynamics. Single molecule studies with AFM. *Microsc. Microanal.* 8: 170–171.
24. Lushnikov, A. Y., A. Bogdanov, and Y. L. Lyubchenko. 2003. DNA recombination: Holliday junctions dynamics and branch migration. *J. Biol. Chem.* 278:43130–43134.
25. Mikheikin, A. L., A. Y. Lushnikov, and Y. L. Lyubchenko. 2006. Effect of DNA supercoiling on the geometry of Holliday junctions. *Biochemistry*. 45:12998–13006.